CrossMark

ORIGINAL ARTICLE

CO_2/CH_4 separation by means of Matrimid hollow fibre membranes

Francesco Falbo[1] · Adele Brunetti[1] · Giuseppe Barbieri[1] · Enrico Drioli[1,2] · Franco Tasselli[1]

Abstract CO_2/CH_4 mixtures separation was investigated using Matrimid®5218 hollow fibre membranes and measuring the membrane flux feeding singly CH_4 and CO_2 and their mixtures, with CH_4 concentration ranging from 5 to 70 %$_{molar}$. Specific attention was paid to membrane properties at a high temperature (up to 75 °C) and feeding humidified streams, not yet particularly investigated, in a pressure range 400–600 kPa. The membrane properties were restored when water vapour was removed and temperature decreased stating the excellent hydro-thermal stability of these membranes. Maps of the separation performance were also calculated for a range of operating conditions wider than the experimental one paying specific attention to the feed/permeate pressure ratio further to membrane selectivity and permeance. Single and multi-stage membrane separation systems were investigated using these maps. The prepared Matrimid®5218 hollow fibres showed very good performance in terms of flux and selectivity for temperatures up to 60 °C, also in steam saturated conditions, allowing a methane concentration meeting the specification for its injection into the grid.

Keywords CO_2/CH_4 separation · Hollow fibre membrane · Matrimid®5218 · Membrane performance maps

✉ Giuseppe Barbieri
g.barbieri@itm.cnr.it

[1] National Research Council-Institute on Membrane Technology (ITM-CNR), Via P. Bucci, cubo 17C c/o Unical, 87036 Rende CS, Italy

[2] The University of Calabria, cubo 44A, Via Pietro BUCCI, 87036 Rende CS, Italy

Introduction

CO_2 is significantly present in mixtures where CH_4 is the major and valuable component. CH_4 is largely utilized fuel for domestic and automotive uses, electricity and power generation, owing to its large production and after its concentration [1]. Natural gas mainly contains CH_4 (60–90 %) and undesired compound such as CO_2 (4–35 %) and H_2O (5–10 %) [2, 3]. CH_4 (50–70 %), CO_2 (30–50 %) and H_2O (5–10 %) are the main components of biogas [4]. The presence of CO_2 not only reduces the calorific power, but increases the costs for gas compression and transport. The removal of CO_2 from CH_4 mixtures is, thus, very important in several industrial processes such as biogas upgrading or natural gas sweetening. To fit the targets for injecting the gas into the natural gas grid [1, 5], CO_2 concentration has to be lowered down to ca. 2–4 % (Table 1) [6–8]. In addition, a cleaning process is required for the removal of the other inert (e.g. N_2), dangerous (e.g. H_2O) and trace of harmful (e.g. H_2S) components for the environment and gas grid (Table 1). Conventional industrial methods used for CO_2 removal include processes such as adsorption [8], water scrubbing [9] and absorption [10].

Usually, the sweetening is achieved by means of absorption with an aqueous alkanolamine solution that has as main drawback the tendency to equipment corrosion and to lose amine properties by degradation increases [11].

As an alternative membrane, separation processes generally offer several advantages over the above-mentioned conventional separation techniques including low capital cost, ease of processing, small footprint area, high energy efficiency and ease of preparation and control [12–14].

To use the membranes, they have to exhibit high separation performance in real condition. Moreover, they have to show important characteristics such as thermal,

مدينة الملك عبدالعزيز للعلوم والتقنية KACST

Springer

Table 1 Targets for injecting the gas into the natural gas grid [1]

Component	Specification		
	Germany	Austria	US
CO_2 (%)	<2–4	<2–4	<2–4
Water	<dew point	<dew point	<120 ppm
H_2S (ppm)	<3	<4	<3.7
O_2 dehydrated gas networks (%)	<3	<4	<0.2–1
O_2 non-dehydrated gas networks (%)	<0.5	<0.5	<0.2–1
Total inert gases (N_2, He) (%)	<4	<4	<4

mechanical, chemical resistance and durability, also in the presence of harsh environments, reproducibility at a high scale level, easy handling, etc., to be suitable for industrial use.

Recently, Basu et al. [9] and Zhang et al. [15] published two reviews reporting the membrane materials used for CO_2/CH_4. Cellulose acetates [6] and polyimides [16, 17] exhibit the best combination of permeability and selectivity. Cellulose acetate-based membranes for CO_2/CH_4 separation have become commercial, since the mid-1980s. These membranes make up to 80 % of the market for membranes in natural gas processing, and because of their wide industrial acceptance have become an industry standard for comparison purposes. Cynara [18] and UOP Separex [19] are the two major membrane manufacturers currently supplying cellulose acetate-based modules as hollow fibres and spiral wound, respectively. However, cellulose acetate membranes are sensitive to water vapour and a stream pre-treatment is necessary to use them for the treatment of these gas streams [7].

Polyimide hollow fibre membranes are an alternative to cellulose acetate, because they combine excellent thermal and chemical stability and show a high water resistance [20] in biogas upgrading. They are commercialized by UBE Industries [21] and Air Liquide Medal [22].

In this work, Matrimid®5218 asymmetric hollow fibre membranes were prepared by means of the phase inversion dry-jet wet spinning technique [23]. The choice of hollow fibre configuration, among the various possible membrane configurations, was made owing to their high surface/volume ratios, excellent mechanical strength, and low production costs and reduced overall size of the equipment (footprint).

Many studies [24–31] can be found in the open literature on the use of polyimides for the membranes preparation; in them, the mass transport proprieties were usually evaluated feeding single gas such as CO_2, CH_4, N_2, H_2, O_2 and mixtures of CO_2/CH_4 or CO_2/N_2 in the temperature range 25–75 °C. Most of the studies were also focalized on the improvement of the separation properties of these

membranes by different blends [24, 25] or the addition of fillers [26–28] or introducing new preparation techniques and post-treatments [29–31] for improving durability and mechanical and thermal resistance.

In addition, in real applications, almost all the streams contain water vapour. Even though, it is usually removed by dehydration processes by upfront units; in this work, it was present in the feed stream also for demonstrating that the water removal step is not a mandatory requirement before the separation of gases, since the membrane does not suffer any problem related to the water present in large concentration too. Such a solution, lowering the flow rate of the stream to be dehydrated, would reduce the amount of water to be removed. Thus, a membrane integrating separation has a freedom degree, for placing the dehydration unit, greater than the one in conventional separation cycles. The effect of vapour on the mass transport properties of the membranes is only partially investigated in the literature since, generally, the majority of studies refers to the transport properties measured in dry condition, usually considering single gases. Chenar et al. [32] and Scholes et al. [33] studied the effect of water vapour on the performance of polyimide hollow fibre membranes at 25–35 °C.

Investigations on mass transport of polyimides membrane coupling humidified feed mixtures with a higher temperature range are still missing in the open literature, at our knowledge. Therefore, this work proposes and discusses separation performance of prepared Matrimid®5218 membranes feeding humidified gas mixture also in the temperature range 50–75 °C.

On the basis of the previous considerations, the hollow fibre membrane transport properties were evaluated using, in addition to single gases and dry condition, humidified CH_4:CO_2 mixtures up to 75 °C. The experiments were carried out in a pressure range of 400–600 kPa which is a typical range of biogas upgrading. The higher pressure required by the natural gas sweetening is beyond the aim of this work.

In addition, the experimental data obtained were used as input data for a simulation analysis devoted to investigate the capability of these membranes to separate/purify methane from these streams. In particular, performance maps were developed with which the purity and recoveries of both retentate and permeate streams were predicted in a wider range of operating conditions with respect to the ones used at laboratory scale.

Materials and experimental methods

Materials

Matrimid®5218 was supplied by Huntsman Advanced Materials American, the Woodlands (USA). *N*-Methyl-2-

Table 2 Operating conditions used for gas separation measurements

Temperature (°C)	25, 50, 60, 75
Pressure (kPa)	Feed/retentate: 400, 500, 600
	Permeate: 100
Feed flow rate	24 dm^3 (STP) h^{-1}
Relative humidity (%)	0, 50 and 100
Feed composition	Single gases: CO_2 (purity of 99.99 %) and CH_4 (purity of 99.99 %)
	CH_4:CO_2 mixtures (molar composition, %) 50:50 70:30 5:95

STP: 0 °C and 100 kPa

pyrrolidone (purity of 99 %) was purchased from VWR International PBI (Italy). The bi-components, Stycast 1266, epoxy resin was used for potting fibres in the preparation of modules, were purchased from Emerson & Cuming (Belgium). Tap water was used as the external coagulant and distilled water was used as the bore fluid. CO_2 and CH_4 used in as single gas had a purity of 99.99 %; they were mixed for producing the mixtures as reported in Table 2.

Hollow fibre preparation

The hollow fibre membranes preparation was carried out according to the dry-jet wet spinning technique. Details on the preparation of the polymer solution (dope), on the spinning setup and on membrane modules were reported in a previous paper [20]. Membrane modules were prepared with the fibres produced, assembling ten fibres 20 cm long for a total membrane area of 52 cm^2. The skin dense layer being on the outer side of the fibres, the membrane area was calculated taking the external diameter of the fibres.

Mass transport properties evaluation

The mass transport properties of the hollow fibre membrane modules were measured with single gases, CH_4 and CO_2, and their mixtures, referred to as molar ratio, CH_4:CO_2 = 50:50, CH_4:CO_2 = 70:30 and CH_4:CO_2 = 5:95. All measurements were carried out at different pressures, temperatures, and relative humidity as reported in Table 2.

During the gas permeation measurements, the modules which have two inputs (feed and retentate) and one output (permeate) were placed in a furnace to keep under control the temperature. The feed and retentate pressures were measured by manometers and their flow rates were measured by bubble soap flow meter.

The gas streams were analysed by an Agilent GC 6890 equipped with two parallel analytical lines, identified as front and back. This means that it was equipped with two sampling valves, two detectors (TCD), and two series of columns (HPLOT + molesieve). The temperature was 120 °C and 150 °C for both front and back sample valves and detectors, respectively. The oven temperature was kept at 50 °C. Column 1, an HPLOT, operated at 123 kPa (17.781 psi) under a carrier gas flow rate of 7.08 mL min^{-1}, whereas column 2, a molesieve, operated at 128 kPa (18.533 psi) under a carrier gas flow rate of 7.5 mL min^{-1}, for each analytical line.

The permeation measurements with single gases were performed using the pressure drop method controlling the pressure by means of a forward pressure controller placed on the feed line.

The mixtures measurements were carried out using the concentration gradient method (Fig. 1) and the retentate and permeate compositions were analysed using a gas chromatograph. In this case, the feed/retentate pressure was controlled by means of a back pressure controller placed on
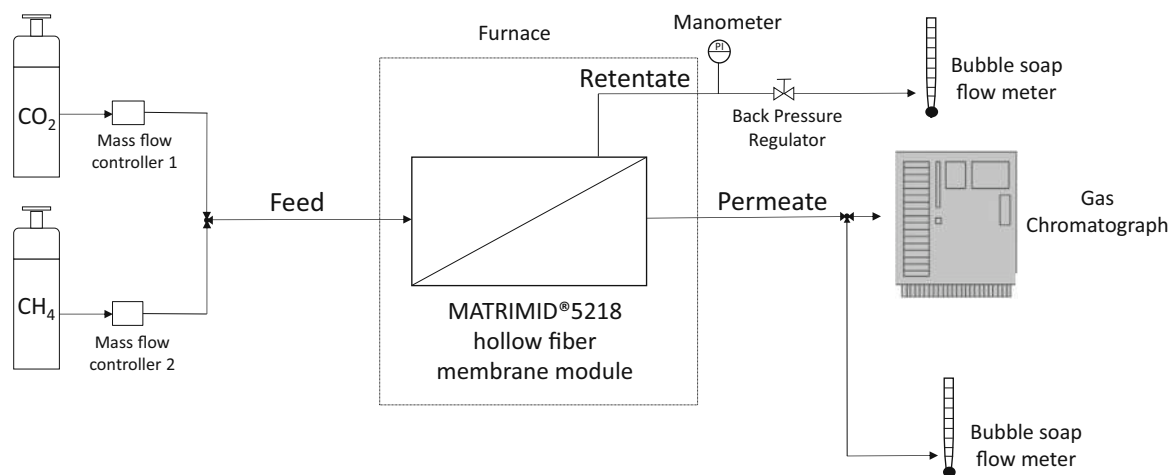
Fig. 1 Scheme of the experimental setup used for mixture measurements

the retentate line. The mixtures were obtained by mixing CO_2 and CH_4 coming from two different cylinders that were fed to the membrane modules by means of two mass flow controllers [34].

All the measurements were carried out by feeding the gas on the outer (shell) side of the fibres and the permeate was collected from the inner hole. The permeate and retentate flow rates were measured by means of two bubble soap flow meters.

In the experiments with water vapour, to obtain 100 % relative humidity, the feed stream, either single gas or mixture, was firstly fed into a humidifier at the same temperature and pressure as the membrane module and then, once saturated, into the module. For the measurements at 50 % relative humidity, a part of the feed streams (50 %) is fed into the humidifier and another part not. The two streams are combined before the module and are then fed to reach 50 % relative humidity. The relative humidity, in both cases, was measured by means of two humidity sensors placed on the feed and permeate lines.

In addition, the modules were placed in oblique position inside the furnace to avoid any liquid deposition also on the external surface of the fibres.

All the measurements were performed at a high feed flow rate Table 2 and, consequently, at a low stage cut, 5–10 %, (ratio of the permeate flow rate to the feed flow rate). This condition assures the absence of variation of the species composition in the feed/retentate side.

The performances of the membranes were evaluated in terms of permeating flux (Eq. 1) and permeance (Eq. 2) where A^{Membrane} (52 cm^2) is the membrane area and the permeation driving force is given by the difference of the species partial pressure on the two membrane sides (Eq. 3). The single gas selectivity and the selectivity in mixture are given by the ratio of the measured permeances (Eq. 4). In addition, the separation factor was also calculated, however, owing to the low stage cut it coincides with the mixture selectivity. The investigated hollow fibres have an asymmetric structure with a selective and thin dense layer on others of different porosity and pore size. The thickness of the selective layer only was utilized in the permeability evaluation as used for symmetric and asymmetric flat films.

$$\text{Permeating flux}_i = \frac{\text{Permeate flow rate}_i}{A^{\text{Membrane}}} \ (\text{mol m}^{-2}\,\text{s}^{-1}) \tag{1}$$

$$\text{Permeance}_i = \frac{\text{Permeanting flux}}{\text{Driving force}} (\text{mol m}^{-2}\,\text{s}^{-1}\,\text{Pa}^{-1}) \tag{2}$$

$$\text{Driving force}_i = P_i^{\text{Feed}} - P_i^{\text{Permeate}} \ (\text{kPa}) \tag{3}$$

$$\text{Selectivity}_{ij} = \frac{\text{Permeance}_i}{\text{Permeance}_j} \tag{4}$$

Tools for membrane system performance analysis

In some previous papers [12, 13], the authors developed a simple tool that uses "maps" to enable analysis of performance and the perspectives of membranes in CO_2 capture. That study focused on the application of membrane gas separation in CO_2 processing with a general approach considering the effect and, eventually, the limitations offered by the main variables that affect the separation performance: the pressure ratio, the feed composition, and the mass transport properties (permeance and selectivity) of the membrane considered in the installation. As performed, the study is a useful guide for readers interested in CO_2 separation independent of the other gases present in the feed stream.

In the dimensionless form of the equations, the terms Θ_i and ϕ can be distinguished as the permeation number and the feed to permeate pressure ratio, respectively.

$$\Theta = \frac{\text{Permeance}_{\text{CO2}} \times A^{\text{Membrane}} \times \text{Feed pressure}}{\text{CO}_2\,\text{feed mole fraction} \times \text{Flow rate}^{\text{Feed}}} \tag{5}$$

$$\phi = \frac{\text{Feed pressure}}{\text{Permeate pressure}} \tag{6}$$

The permeation number (Eq. 5) expresses a comparison between the two main transport mechanisms involved that are the convective flux along the membrane axis and the maximum permeating flux achievable. A high permeation number corresponds to a high membrane area and/or permeance for the stream and to a high permeation through the membrane with respect to the total flux along the module. The pressure ratio (Eq. 6) is one of the most important and determinant operating parameters affecting the performance of the membrane unit and is the driving force for the separation. More details about the model used and the dimensionless analysis can be found in [12].

Results and discussion

Measurements feeding single gases

The permeating flux was measured up to 75 °C to evaluate the suitability of the prepared membranes for the targeted separation at a relative high temperature.

Figure 2 shows the CH_4 and CO_2 permeating flux as a function of the driving force at 60 °C. Both CO_2 and CH_4 fluxes linearly increased indicating that the permeance of each gas was constant for all the applied values of the driving force. CO_2 flux was always greater than that CH_4 since CO_2 higher solubility in Matrimid®5218 membrane with respect to CH_4 one. The difference in permeance of CO_2 and CH_4 can be explained on the basis of difference in
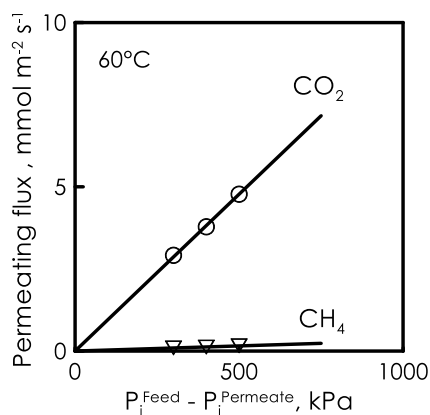
Fig. 2 CH_4 and CO_2 permeating flux measured for single gases as a function of the driving force. Feed pressure range 400–600 kPa and permeate pressure 100 kPa. *Solid lines* linear correlation of experimental data

Fig. 3 CO_2 and CH_4 permeance and CO_2/CH_4 single gas selectivity as a function of temperature. Feed pressure range 400–600 kPa and permeate pressure 100 kPa. Experimental measurements (*symbols*) and *lines* connecting experimental data

the gas–polymer interaction. CO_2 has both a higher solubility and diffusivity than methane (Table 3). For comparing the mass transport properties measured in this work with those available in the literature on the same membrane type, the permeability of hollow fibre membrane is calculated considering the separating layer thickness of 0.4 μm. It resulted from an estimation carried out on SEM images of the cross section of several hollow fibre samples. This comparison gives quite good agreement both in terms of permeability (2.71 versus 2.76 and 0.080 versus 0.081 for CO_2 and CH_4, respectively) and CO_2/CH_4 selectivity which is 34.0 and 34.1 from the literature and developed membranes, respectively.

The same linear behaviour of the permeating flux was also observed at 25, 50 and 75 °C; then, CO_2 and CH_4 permeance at all the investigated temperature were calculated using the Eq. (2). Figure 3 shows as the permeance of both gases increases with the temperature, the permeation being an activated mechanism following the Arrhenius law.

CO_2 permeance increased quite linearly (apparently, owing to the Arrhenius plot) with the temperature up to 75 °C, the highest temperature value analysed, whereas for

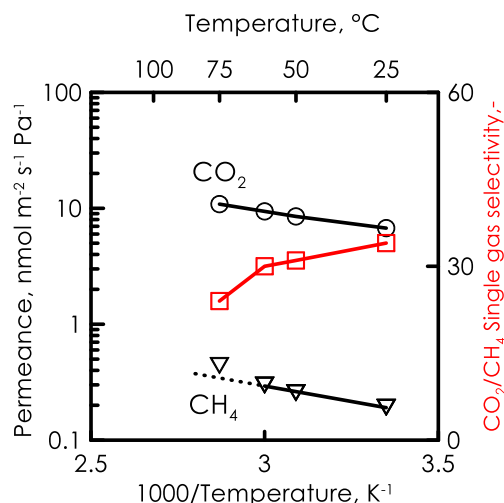CH_4 the linear trend was kept up to 60 °C. In fact, CH_4 permeance value at 75 °C exceeded the prevision given by the linear trend crossing the permeance at the lower temperatures. The temperature dependency of permeability results as a combination of diffusion and sorption components which increases and decreases with the temperature, respectively. However, the evaluation of these components disregards the purpose of this work.

The prepared membrane showed CO_2/CH_4 selectivity decreasing in the range of temperature investigated (Fig. 3) keeping a high value between 34 and 31 up to 60 °C. It dropped to 24, a still interesting value, at 75 °C. It is worth to notice that the performance of the membranes was restored when the temperature was reduced.

Measurements feeding dry gas mixtures

Three CH_4–CO_2 mixtures (molar composition of 5:95; 50:50 and 70:30, Table 2) were fed to the membrane module kept at a constant temperature up to 75 °C.

Table 3 Solubility and diffusivity in Matrimid®5218 membranes at 35 °C as reported by [35] and permeance *thickness as measured at 25 °C in this work

	As reported by [35]			This work
	Solubility (cm^3) (at 25 °C)/cm^3 cmHg	Diffusivity (cm^2 s^{-1})	Permeability** (femto-mol m^{-1} s^{-1} Pa^{-1})	Permeability* (femto-mol m^{-1} s^{-1} Pa^{-1})
CO_2	31.0×10^{-3}	2.85×10^{-8}	2.71 (88.4×10^{-11})	2.76
CH_4	2.5×10^{-3}	1.04×10^{-8}	0.080 (2.6×10^{-11})	0.081
CO_2/CH_4 selectivity (–)			34.0	34.1

* Calculated considering a separating layer thickness of 0.4 μm

** Calculates as solubility × diffusivity

Fig. 4 Permeating flux of CO_2 and CH_4 and in mixture as a function of the driving force. Feed pressure range 400–600 kPa and permeate pressure 100 kPa. Experimental measurements (*symbols*) and linear correlation of experimental data
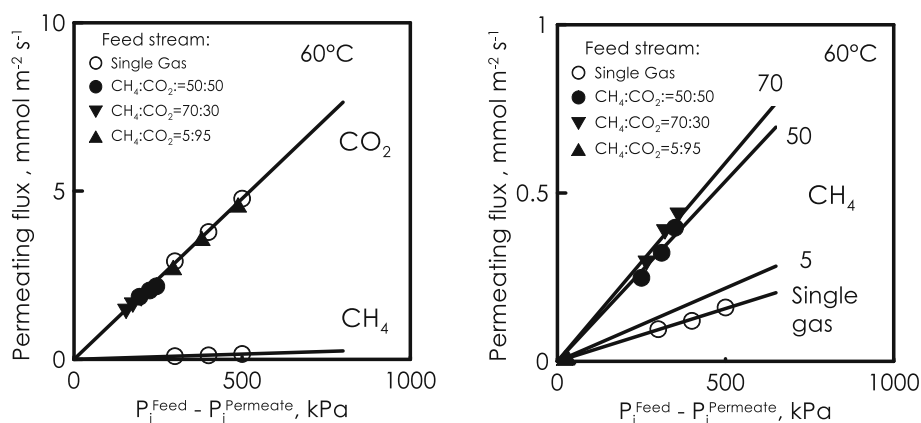

Figure 4 shows the permeating flux of CO_2 and CH_4 feeding the mixtures as a function of the driving force at 60 °C. Single gas values are also shown for comparison reasons. A linear dependence of the fluxes on the driving force was observed for both species at all the temperatures including 75 °C. No change in CO_2 permeance as function of feed composition was observed with respect to the single gas measures: all the measurements (single gas or gas mixtures) are aligned on the same line. On the contrary, the CH_4 permeance (Fig. 4, right side) changes with the feed concentration as detailed in Table 4.

The CH_4 sorption in the Matrimid has a specific value and in the ternary system (CO_2–CH_4–Matrimid) the influence of CO_2 has to be taken into account also on this parameter. The presence of CO_2 is expected to reduce CH_4

sorption, since CO_2 competes with CH_4. Minelli et al. [36] calculating CH_4 sorption as a decreasing function of the CO_2 concentration for polyphenylene oxide and poly-methylmetacrylate confirmed the competitiveness of the absorption of the two gases. Scholes et al. [37] focused on CO_2 and CH_4 competitive sorption in a Matrimid membrane. Lin and Yavari [38] simulated on a free volume-based model the decreasing trend of CO_2/CH_4 selectivity in mixture. As experimentally observed, CO_2 promotes CH_4 permeation; its concentration of 30–50 $\%_{molar}$ in the feed mixtures is probably enough to significantly reduce the CH_4–Matrimid interactions (sorption) with respect to CH_4 when fed alone. This should increase, in the meantime, methane diffusion probably owing to the combination of two potential effects: (1) a small swelling of the membrane owing to CO_2 sorption and (2) a facilitated diffusion of CH_4 inside the membrane bulk where polymer chains are partly covered by CO_2 sorbed on them. The overall effect results in a higher CH_4 permeance. A selectivity loss was consequently observed. When CO_2 concentration is 95 $\%_{molar}$, the methane is too low (5 $\%_{molar}$) for showing a permeance increase.

A similar trend was observed by Lin and Yavari [38], by Houde et al. [39] and Scholes et al. [37], who confirmed the competitive sorption between CO_2 and CH_4 (Table 5) in cellulose acetate, polyphenilene oxide and polyimmide,

Table 4 CH_4 permeance measured in mixtures at 60 °C as a function of CH_4 feed concentration

CH_4 feed concentration ($\%_{molar}$)	CO_2 feed concentration ($\%_{molar}$)	CH_4 permeance (pico-mol m^{-2} s^{-1} Pa^{-1})
100	0	300
5	95	310
50	50	370
70	30	390

Table 5 CO2/CH4 selectivity in mixture at 35 °C

Membrane material	CO_2/CH_4 selectivity (–)			Reference
	Single gas	Mixture		
Cellulose acetate	35	$CH_4:CO_2 = 20:80$ 20	$CH_4:CO_2 = 80:20$ 25	Lin et al. [38]
Polyimide	49	$CH_4:CO_2 = 90:10$ 41		Scholes et al. [37]
Polyphenylene oxide	42	$CH_4:CO_2 = 90:10$ 29	$CH_4:CO_2 = 76:24$ 35	Houde et al. [39]

Fig. 5 CO_2 and CH_4 permeance and CO_2/CH_4 selectivity in mixtures as a function of temperature. Feed pressure range 400–600 kPa and permeate pressure 100 kPa. Experimental measurements (*symbols*) and *lines* connecting experimental data
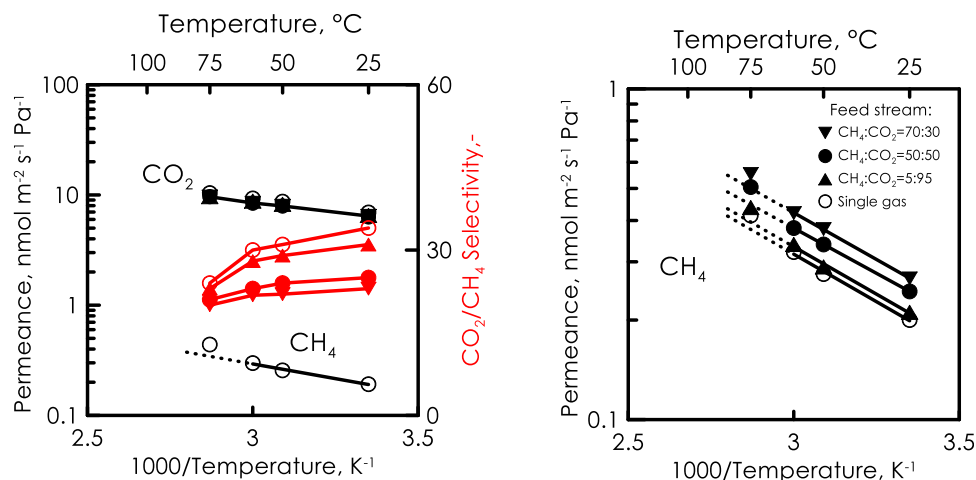
respectively; CO_2 plasticization which causes membrane swelling also plays a crucial role. The CO_2/CH_4 selectivity value in mixtures was lower for ca. 35 % than that obtained for the single gas. CO_2 permeance, mainly owing to CO_2 solubility (and not its diffusion), does not undergo a significant change and CO_2 permeates the membrane in the same way fed singly or in a gas mixture. Differently, CH_4 permeance benefits of the swelling effects with consequent diffusion increase.

The same behaviour was also observed at the other investigated temperatures including 75 °C.

The permeance of CO_2 and CH_4 as a function of the temperature (Fig. 5) shows the same apparently linear (owing to the Arrhenius plot) trend already observed for single gas (Fig. 3) confirming the obedience to the Arrhenius law. Furthermore, the selectivity measured when using mixtures (Fig. 5) shows the same trend as that obtained with single gases. It is lower in relation to the higher CH_4 concentration of the feed mixtures. In the whole temperature range analysed, the values of the selectivity measured with mixture were lower than the single gas selectivity.

The low stage cut (5-10 %) set in the experimental measurements means that the differences between the mixture selectivity and the single gas selectivity cannot be attributed to the eventual presence of partial pressure profiles along the module length, but only to the interactions occurring among gases and membrane.

Figure 6 shows CH_4 retentate concentration as a function of CH_4 feed concentration at the three different feed pressures investigated (400, 500, 600 kPa) at 50 °C feeding dry gas. CH_4 concentration in the retentate increased with the concentration of CH_4 in the feed streams. Under the same experimental conditions feeding a mixture with a major concentration of CH_4 in the feed stream a higher CH_4 retentate concentration was observed. The increase of CH_4 concentration in the retentate was also directly related
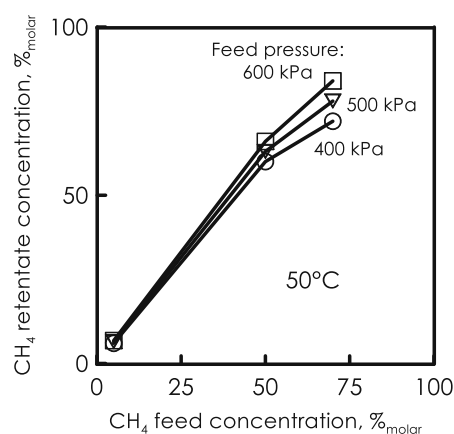

Fig. 6 CH_4 retentate concentration as a function of the CH_4 feed concentration at the three different feed pressures investigated feeding dry mixtures. Experimental measurements (*symbols*) and *lines* connecting experimental data

to the feed pressure and, consequently, also to the driving force. This behaviour is particularly evident at a high feed concentration of CH_4. In fact, with a feed mixture containing 70 $\%_{molar}$ of CH_4, the retentate composition increased from ca. 75 to ca. 90 $\%_{molar}$ at feed pressure of 400 and 600 kPa, respectively. These results indicate that with a feed stream composition similar to that of biogas (see Introduction), it is possible with a single stage membrane operation, to obtain a gas mixture potentially injectable into the grid of CH_4.

A similar trend of CO_2 concentration is evident in the permeate stream in Fig. 7. As experimentally observed, CO_2 concentration increases with the feed pressure. The driving force allowing the molecules permeation directly depends on the feed pressure and, consequently with the driving force, increases CO_2 permeate concentration too. The strongest increase of CO_2 concentration is obtained at 600 kPa at the lowest CO_2 concentration (30 $\%_{molar}$) in the
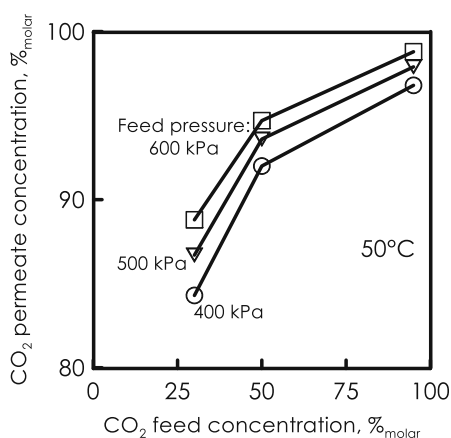
Fig. 7 CO_2 permeate concentration as a function of the CO_2 feed concentration at the three different feed pressures investigated (400, 500, 600 kPa) at 50 °C feeding dry mixtures. Experimental measurements (*symbols*) and *lines* connecting experimental data

Fig. 8 CO_2 and CH_4 permeance in mixtures CH_4:CO_2 = 50:50 (*left side*) and CH_4:CO_2 = 70:30 (*right side*) as a function of relative humidity at the two temperatures investigated (25 and 75 °C). Feed pressure range 400–600 kPa, permeate pressure 100 kPa. Experimental measurements (*symbols*) and *lines* connecting experimental data

feed stream. For the feed mixture at 50 %$_{molar}$ CO_2, the CO_2 permeate concentration was ca. 95 %$_{molar}$ at a feed pressure of 600 kPa. These results are very interesting since the high CO_2 permeate concentration is the fundamental requirement for the capture and storage of the CO_2 streams. The CO_2 capture by means of membrane could be identified as one potential solution to reduce greenhouse gas emissions which causes climate change.

Measurements feeding humidified gas mixtures

Most often the permeation measurements are carried out with dry gas. However, most of the industrial streams to be treated contain a large amount of water vapour, thus membrane performances are affected by it. Indeed, to better evaluate the membrane module application for CO_2/CH_4 mixture separation, experimental measurements using CO_2/CH_4 mixtures humidified at different values of relative humidity (50 and 100 %) were carried out.

Figure 8 shows the CO_2 and CH_4 permeance, feeding CH_4:CO_2 = 50:50 (left side) and CH_4:CO_2 = 70:30 (right side) mixtures, as a function of relative humidity at 25 and 60 °C. In both mixtures, the water influenced the transport properties of the membrane modules by inducing a decrease in permeance of the two gases as the relative humidity increased. The same behaviour was also observed at 75 °C.

From 0 to 50 % of relative humidity, the CO_2 permeance decrease was only ca. 10 % whereas for CH_4 it was ca. 5 % for all the temperatures investigated. This result is interesting because 50 % relative humidity does not change the transport property of the membrane significantly.

From 50 to 100 % relative humidity, the permeance decrease was larger, being ca. 40 % for CO_2 and ca. 20 %
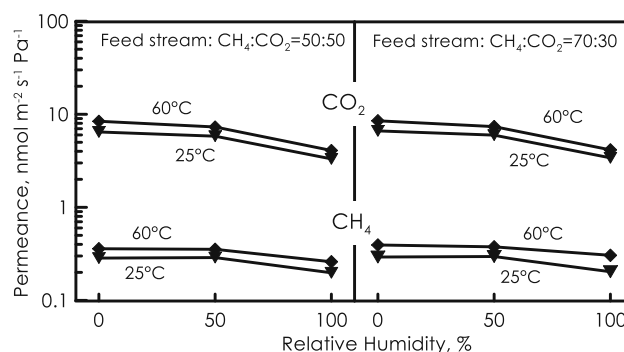
for CH_4. This different trend, between CO_2 and CH_4, could be attributed to the different solubility of CO_2, CH_4 and water in the polymeric matrix. As Scholes et al. [37] and Li et al. [38] demonstrated, water is the more soluble species (0.4 cm^3 STP/cm^3 cmHg at 35 °C) and its molecules fill the sorption sites available, present between the polymeric chains, used by CO_2 or CH_4 for passing through the membrane. Also CO_2 has a good solubility (28×10^{-3} cm^3 STP/cm^3 cmHg at 35 °C) even though significantly lower than that of water; therefore, it can fill only the sites not occupied by water when competitive sorption of both occurs. The reduced CO_2 sorption produces a lower permeation of this species. CH_4 solubility (2.5×10^{-3} cm^3 STP/cm^3 cmHg at 35 °C) is much lower in the polymeric matrix, consequently also its sorption and thus permeance significantly reduces. The same behaviour was observed for both mixtures and the effect on the selective properties is illustrated in Fig. 9 where CO_2/CH_4 selectivity is shown as a function of the relative humidity, at 25 and 60 °C feeding CH_4:CO_2 = 50:50 and CH_4:CO_2 = 70:30 on left and right sides, respectively. In both cases, the selectivity decreases with the relative humidity. The decreasing was not so significant at 50 % relative humidity but was more evident in vapour-saturated condition. The same behaviour was also observed at 50 and 75 °C.

However, for the mixture CH_4:CO_2 = 50:50, CO_2/CH_4 selectivities were very interesting with values between 25 and 18 and in the range 18–13 at 25 and 75 °C, respectively. For the CH_4:CO_2 = 70:30 mixture, the selectivity was between 23 and 17 at 25 °C and between 13 and 11 at 75 °C.

It is important to notice that the performance of the membranes was restored when the water vapour was removed. These results show that the membrane module
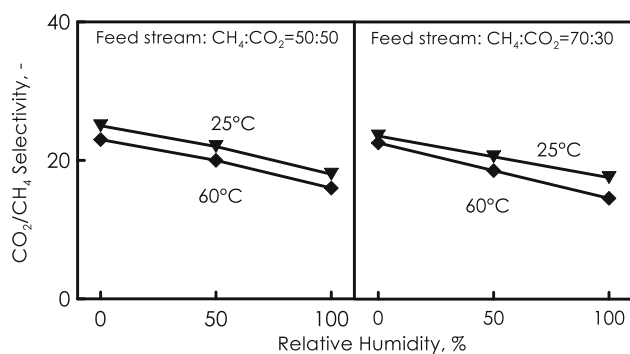
Fig. 9 Selectivity in mixture for $CH_4:CO_2 = 50:50$ (*left side*) and $CH_4:CO_2 = 70:30$ (*right side*) as a function of relative humidity at the two temperatures investigated (25 and 60 °C). Feed pressure range 400–600 kPa, permeate pressure 100 kPa. Experimental measurements (*symbols*) and *lines* connecting experimental data
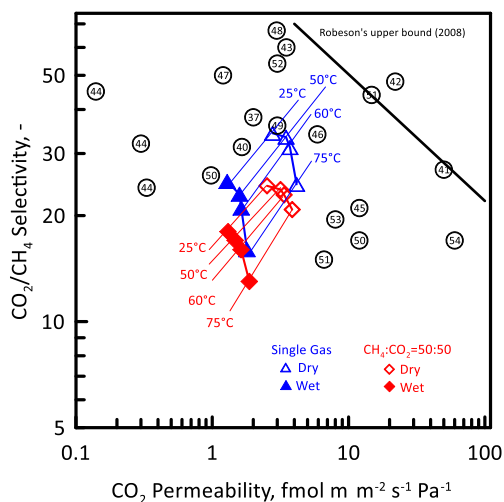

Fig. 10 CO_2/CH_4 single gas selectivity or mixture selectivity of gases measured as a function of the CO_2 permeability; Symbols: *triangles* and *diamonds* refer to experimental data; *circles* refer to the literature data: Ayala et al. [40]; Xiao et al. [41]; Chan et al. [42]; Staudt Bickel et al. [43]; Peter et al. [44]; Shao et al. [45]; Hillock et Koros [46]; Suzuki et al. [47]; Swaidan et al. [48]; Sanders et al. [49]; Vinh-Thang et al. [50]; Nik et al. [51]; Qui et al. [52]; Hosseini et al. [53]; Askari et al. [54]; Scholes et al. [37]

developed can separate the CH_4 from CO_2 in the presence of water vapour.

A wide comparison of mass transport properties measured in this work with those currently available in the open literature, the state of the art (the Robeson's upper-bound), can be done only through the permeability. Thus, the permeability was calculated considering the separating layer thickness of 0.4 µm, as estimated by SEM analysis. Figure 10 compares the mass transport properties measured in this work, with the current state of art on the Matrimid®5218 and polyimide, a material similar to Matrimid®5218.

The better results in terms of selectivity and permeance were obtained for the single gas measurements. There was no change in CO_2 permeance feeding single gas or a gas mixture. A reduction of selectivity of ca. 20 % was observed when a dry $CH_4:CO_2 = 50:50$ mixture was fed. The membrane selectivity was reduced of ca. 25 and 50% in presence of 50 and 100 % of relative humidity in the feed stream, respectively. Permeability and selectivity of the developed membranes were lower than the better values (ca. 50 as selectivity and ca. 20 nmol m^{-2} s^{-1} Pa^{-1} as CO_2 permeance) of literature data of 6FDA-based polyimides. However, the membranes prepared in this work show interesting gas transport properties, also a temperature of 75 °C and feeding dry and humidified streams. In particular, CO_2/CH_4 selectivity in the range of 34–24 and 25–21 was obtained feeding dry single gas and dry mixture, respectively. In humidified conditions, the CO_2/CH_4 selectivity was between 25 and 12 and between 18 and 13 feeding single gas and mixture, respectively. It is important to notice that the performance of the membranes was restored when the water vapour was removed and when the temperature was reduced.

Some remarks on the membrane system performance

One of the main points of discussion which often interfaces material scientists with process engineers is the possibility of using the materials produced and that gave interesting performance in mixtures in the laboratory. Apart from the necessity to test the performance in mixtures, a crucial role for the application of membrane technology in CO_2 separation is played by the membrane engineering who knows how to operate the membrane unit and to design the separation process to obtain the best performance. By means of the performance maps developed elsewhere, it is possible to elaborate a predictive analysis of the membrane unit performance in a wider range of operating conditions.

Figure 11 shows the CO_2 permeate concentration versus recovery for different values of feed compositions experimentally tested at various values of pressure ratio and permeation number.

Once, on the basis of global economic considerations the optimal performance (that is, a point on the plot of CO_2 permeate concentration versus CO_2 recovery) has been chosen, it can be univocally individuated on the maps; the parametric curves crossing this optimal point provide the corresponding pressure ratio and permeation number. This leads to the identification of the operating conditions, membrane characteristics (permeance, area, etc.), or feed conditions required to obtain the final product with certain characteristics.
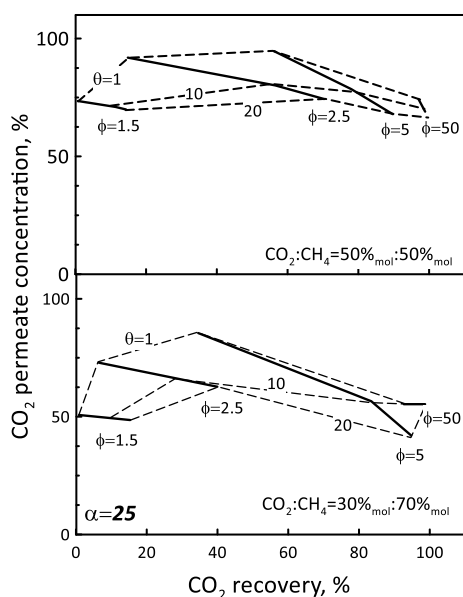
Fig. 11 Maps of CO_2 concentration in permeate streams, respectively, as a function of recovery at various values of pressure ratio and permeation number

For instance, if 60 %$_{molar}$ CO_2 recovery in the permeate is desired, the pressure ratio required is close to 2.5 in the case of the equimolecular mixture (CH_4:CO_2 = 50:50), whereas it increases to 5 for the mixture with the higher concentration of methane (CH_4:CO_2 = 70:30). Assuming this latter as reference mixture, for a pressure ratio of 5, the CO_2 concentration in the permeate can range between 50 to more than 80 to 90 %$_{molar}$, according to the permeation number chosen with consequent changes on the recovery which can pass from 80 down to 40 %$_{molar}$, respectively.

Following the indications of the International Energy Agency [55–58] for which a purity higher than 80 %$_{molar}$ and a recovery >60 %$_{molar}$ are desirable targets, the permeation number selected should be close to 1. For defined feed conditions and membrane characteristics, it is possible to calculate the membrane area required to treat certain feed flow rates. At a greater pressure, the ratio would correspond to a reduction in membrane area.

Apart from the details of the calculation, it appears evident that in a single stage the proposed membranes cannot contemporarily reach high recovery and purity. However, this analysis provides an indication on the possibility of using these membranes as the first stage in a multistage system to concentrate the feed stream or as a single stage unit when the recovery target is not important.

In the case of biogas separation or natural gas sweetening, still much more important than the CO_2 characteristics are the characteristics of the methane stream which remains as retentate. The treatment of these gas streams leads not only to the recovery and sequestration of CO_2, but also to much greater purification and recovery of value-
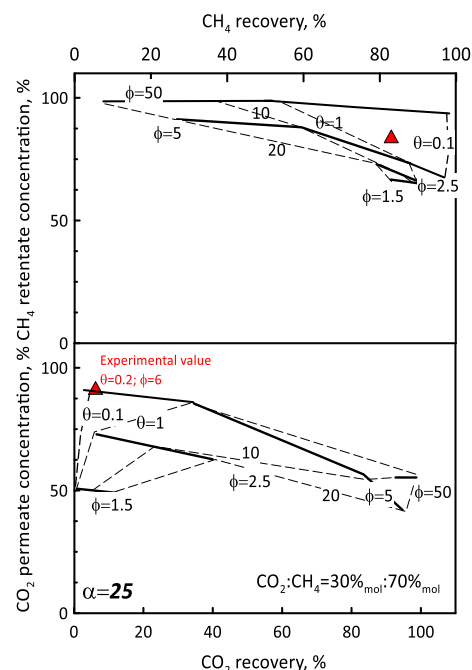

Fig. 12 Maps of CH_4 and CO_2 concentration in retentate and permeate streams, respectively, as a function of correspondent recovery at various values of pressure ratio and permeation number

added CH_4 to feed it directly to pipelines for domestic or stationary uses. From this perspective, since CH_4 has to be fed to pipelines at a high pressure, the possibility of installing a compressor before the membrane system and recovering the methane already concentrated and compressed as a retentate stream makes this operating option quite realistic. Figure 12 depicts the performance map not only for CO_2 characteristics but also for CH_4 ones. From the figure, the advantage achieved both in terms of purity and recovery when a high pressure ratio can be used appears evident. For example, at $\phi = 50$, it is possible to obtain a CH_4 purity greater than 97 %, the limit imposed for directly feeding in pipelines, even though with recovery not so high (ca. 50 %$_{molar}$ for a permeation number equal to 1). To this corresponds a CO_2 recovery greater than 90 % but with a CO_2 concentration of ca. 55 %, at all permeation numbers considered. This stream would require a further separation treatment to fit the indications imposed for CO_2 storage; therefore, a multistage cascade system has to be applied for this solution.

Conclusions

The transport properties of Matrimid®5218 hollow fibre membranes prepared by dry-jet wet spinning were evaluated by feeding singly CH_4 and CO_2 and as CH_4–CO_2 mixtures (of molar composition of 50:50, 70:30 and 5:95).

Specifically, relatively high temperatures for polymeric membranes up to 75 °C and wet condition were operated in measuring the membrane separation properties.

The permeation measurements in the range 25–60 °C showed CO_2/CH_4 selectivity values between 34 and 31 and between 30 and 23 feeding single gases or gas mixtures, respectively. At 75 °C, no difference in CO_2 permeance was observed feeding the different streams, whereas the permeance of CH_4, the less permeating specie, was little higher feeding a mixture stream than that measured as single gases; consequently, the membrane selectivity ranges 22–13 when feeding mixtures. Good CO_2 and CH_4 permeance and selectivity measured up to 75 °C and under water vapour presence. In addition, the membrane properties were restored when water vapour was removed and temperature decreased stating the excellent hydro-thermal stability of these membranes.

The membrane, in fact, shows very good water vapour resistance (50 and 100 % as relative humidity) even though a loss in CO_2/CH_4 selectivity (e.g. 22 at 25 °C; and 11 at 75 °C) was observed. The water vapour, owing to its high solubility in the polymeric matrix, also causes a permeance decrease of 50 and 25 % (at 100 % of relative humidity) of CO_2 and CH_4, respectively.

The measurements in the presence of water vapour (50 and 100 % relative humidity) showed water resistance and a certain loss of selectivity, although not so significant. The measurements also highlight a really good thermal stability because the performance of the membrane was restored when the temperature decreased.

Performance maps calculated for the specific case in a wider range of operating conditions with respect to the ones analysed in laboratory foresee the possibility of using these membranes both as the first stage for stream concentration in a multi-stages system or as single stage membrane unit, particularly when high pressure ratio can be applied.

References

1. Abatzologlou N, Boivin S (2009) A review of biogas purification processes. Biofuels Bioprod Biorefining 3:42–71

2. Boehm P, Saba T (2009) Identification of natural gas sources using geochemical forensic tools. Expon Env Forens Notes 5:1–5

3. Scholes CA, Stevens GW, Kentish SE (2012) Membrane gas separation applications in natural gas processing. Fuel 96:15–28

4. Anderson C (2011) Landfill gas upgrading to pipeline quality in the US, World Congress of Bioenergy, Dalian, China

5. Baker R, Lokhandawala K (2008) Natural gas processing with membranes: an overview. Ind Eng Chem Res 47:2109–2121

6. Bounaceur R, Lape N, Roizard D, Vallieres C, Favre E (2006) Membrane processes for post-combustion carbon dioxide capture: a parametric study. Energy 31:2556–2570

7. Datta AK, Sen PK (2006) Optimization of membrane unit for removing carbon dioxide from natural gas. J Membr Sci 283:291–300

8. Drioli E, Romano M (2001) Progress and new perspectives on integrated membrane operations for sustainable industrial growth. Ind Eng Chem Res 40:1277–1281

9. Basu S, Khan AL, Cano-Odena A, Liu C, Vankelecom IFJ (2009) Membrane-based technologies for biogas separations. Chem Soc Rev 39(2):750–768

10. Tuinier MJ, van Sint Annaland M, Kramer GJ, Kuipers JAM (2010) Cryogenic CO_2 capture using dynamically operated packed beds. Chem Eng Sci 65:114–121

11. Aliabad ZH, Mirzaei S (2009) Removal of CO_2 and H2S using aqueous alkanolamine solusions. World Acad Sci Eng Technol 3:1–25

12. Brunetti A, Scura F, Barbieri G, Drioli E (2010) Membrane technologies for CO_2 separation. J Membr Sci 359:115–125

13. Brunetti A, Drioli E, Lee YM, Barbieri G (2013) Engineering evaluation of CO2 separation by membrane gas separation systems. J Membr Sci 454:305–315

14. Brunetti A, Sun Y, Caravella A, Drioli E, Barbieri G (2015) Process intensification for greenhouse gas separation from biogas: more efficient process schemes based on membrane-integrated systems. Int J Greenh Gas Control 35:18–29

15. Zhang Y, Sunarso J, Liu S, Wang R (2013) Current status and development of membranes for CO_2/CH_4 separation: a review. Int J Greenh Gas Control 12:84–107

16. Jeon YW, Lee DH (2015) Gas membranes for CO_2/CH_4 (biogas) separation: a review. Environ Eng Sci 32(2):172–184

17. Sazali N, Harun Z (2015) Gas permeation properties of the Matrimid based carbon tubular membrane: the effect of carbonization temperature. Int J Concept Mech Civil Eng 31:2357–2760

18. Cameron (2010) CYNARA_CO2 membrane separation solutions. TC9814-012. USA. https://cameron.slb.com/products-and-services/separation-processing-and-treatment/gas-processing-andtreatment/acid-gas-treatment-and-removal/cynara-co2-separation-systems. Accessed 27 June 2016

19. UOP LLC Separex^{TM} (2009) membrane technology. UOP 5241E-01. url:http://www.slideshare.net/hungtv511/uopseparex-membrane-technology. Accessed 27 June 2016

20. Falbo F, Tasselli F, Brunetti A, Drioli E, Barbieri G (2014) Polyimide hollow fiber membranes for CO_2 separation from wet gas mixtures. Braz J Chem Eng 31(4):1023–1034

21. UBE Expands Gas Separation Membrane Production (2006) Membr technol 11:4–5. doi:10.1016/S0958-2118(06)70831-X

22. Air Liquide to Install ASU for Dongbei Special Steel Group (2007) China chemical reporter

23. Choi S, Jansen JC, Tasselli F, Barbieri G, Drioli E (2010) In-line formation of chemically cross-linked P84® co-polyimide hollow fibre membranes for H$_2$/CO$_2$ separation. Sep Purif Technol 76(2):132–139

24. Madaeni SS, Mohammadi NR, Vatanpour V (2012) Preparation and characterization of polyimide and polyethersulfone blend membrane for gas separation. Asia Pac J Chem Eng 7:747–754

25. Loloei M, Moghadassi A, Omidkhah M, Amooghin AE (2015) Improved CO$_2$ separation performance of Matrimid®5218 membrane by addition of low molecular weight polyethylene glycol. Greenh Gas Sci Technol 5:1–15

26. Askari M, Chung TS (2013) Natural gas purification and olefin/paraffin separation using thermal crosslinkable co-polyimide/ZIF-8 mixed matrix membranes. J Membr Sci 444:173–183

27. Diestel L, Wang N, Schulz A, Steinbach F, Caro J (2015) Matrimid-based mixed matrix membranes: interpretation and correlation of experimental findings for zeolitic imidazolate frameworks as fillers in H$_2$/CO$_2$ separation. Ind Eng Chem Res 54:1103–1112

28. Dorosti F, Omidkhah M, Abedini R (2014) Fabrication and characterization of Matrimid/MIL-53 mixed matrix membrane for CO$_2$/CH$_4$ separation. Chem Eng Res Des 92(11):2439–2448

29. Rahmania MR, Kazemib A, Talebniaa F, Khanbabaeib G (2014) Preparation and characterization of cross-linked Matrimid membranes for CO$_2$/CH$_4$ separation. Polym Sci 56(5):650–656

30. Ansaloni L, Minelli M, Baschetti MG, Sarti GC (2015) Effects of thermal treatment and physical aging on the gas transport properties in Matrimid®. Oil Gas Sci Technol 70(2):367–379

31. Salleh WNW, Isa NAIM, Sazali N, Ismail AF (2014) Preparation and characterization of Matrimid-based carbon membrane supported on tube for CO$_2$ separation. Adv Mater Res 1025–1026:770–775

32. Chenar MP, Soltanieh M, Matsuura T, Tabe-Mohammadi A, Khulbe KC (2006) The effect of water vapor on the performance of commercial polyphenylene oxide and Cardo-type polyimide hollow fiber membranes in CO$_2$/CH$_4$ separation applications. J Membr Sci 285:265–271

33. Chen GQ, Scholes CA, Qiao GG, Kentish SE (2011) Water vapor permeation in polyimide membranes. J Membr Sci 379:479–487

34. Brunetti A, Simone S, Scura F, Barbieri G, Figoli A, Drioli E (2009) Hydrogen mixture separation with PEEK-WC asymmetric membranes. Sep Purif Technol 69:195–204

35. Li X, Wang M, Wang S, Li Y, Jiang Z, Guo R, Wu H, Cao XZ, Yang J, Wang B (2015) Constructing CO$_2$ transport passageways in Matrimids membranes using nanohydrogels for efficient carbon capture. J Membr Sci 474:156–166

36. Minelli M, Campagnoli S, De Angelis MG, Doghieri F, Sarti GC (2011) Predictive model for the solubility of fluid mixtures in glassy polymers. Macromolecules 44:4852–4862

37. Scholes AC, Stevens GW, Kentish SE (2012) Membrane gas separation applications in natural gas processing. Fuel 96:15–28

38. Lin H, Yavari M (2015) Upper bound of polymeric membranes for mixed-gas CO$_2$/CH$_4$ separations. J Membr Sci 475:101–109

39. Houde AY, Krishnakumar B, Charati SG, Stern SA (1996) Permeability of dense (homogeneous) cellulose acetate membranes to methane, carbon dioxide, and their mixtures at elevated pressures. J Appl Polym Sci 62:2181–2192

40. Ayala D, Lozano AE, de Abajo J, Garcia-Perez C, de la Campa JG, Peinemann KV, Freeman BD, Prabhakar R (2003) Gas separation properties of aromatic polyimides. J Membr Sci 215:61–73

41. Xiao Y, Chung TS, Guan HM, Guiver MD (2007) Synthesis, cross-linking and carbonization of co-polyimides containing internal acetylene units for gas separation. J Membr Sci 302:254–264

42. Chan SS, Chung TS, Liu Y, Wang R (2003) Gas and hydrocarbon (C$_2$ and C$_3$) transport properties of co-polyimides synthesized from 6FDA and 1,5-NDA(naphthalene)/durene diamines. J Membr Sci 218:235–245

43. Staudt-Bickel C, Koros WJ (1999) Improvement of CO$_2$/CH$_4$ separation characteristics of polyimides by chemical crosslinking. J Membr Sci 155:145–154

44. Peter J, Khalyavina A, Krız J, Bleha M (2009) Synthesis and gas transport properties of ODPA-TAP-ODA hyperbranched polyimides with various comonomer ratios. Euro Polym J 45:1716–1727

45. Shao L, Chung TS, Goh SH, Pramoda KP (2005) The effects of 1,3-cyclohexanebis(methylamine) modification on gas transport and plasticization resistance of polyimide membranes. J Membr Sci 267:78–89

46. Hillock AM, Koros WJ (2007) Cross-linkable polyimide membrane for natural gas purification and carbon dioxide plasticization reduction. Macromolecules 40:583–587

47. Suzuki T, Yamada Y, Sakai J, Itahashi K (2010) Physical and gas transport properties of hyperbranched polyimide–silica hybrid membranes. In: Yampolskii Y, Freeman B (eds) Membrane gas separation. Wiley, Singapore, pp 143–158

48. Swaidan R, Ghanem B, Litwiller E, Pinnau I (2015) Effects ofhydroxyl-functionalization and sub-Tg thermal annealing on high pressure pure-and mixed-gas CO$_2$/CH$_4$ separation by polyimide membranes based on 6FDA and triptycene- containing dianhydrides. J Membr Sci 475:571–581

49. Sanders DE, Smith ZP, Guo RL, Robeson LM, McGrath JE, Paul DR, Freeman BD (2013) Energy-efficient polymeric gas separation membranes for a sustainable future: a review. Polymer 54:4729–4761

50. Vinh-Thang H, Kaliaguine S (2011) MOF-based mixed matrix membranes for industrial applications. In: Ortiz OL, Ramirez LD (eds) Coordination polymers and metal organic frameworks. Nova Science Publishers, Hauppauge NY USA, pp 1–38

51. Nik OG, Chen XY, Kaliaguine S (2012) Functionalized metal organic framework polyimide mixed matrix membranes for CO$_2$/CH$_4$ separation. J Membr Sci 413–414:48–61

52. Qiu W, Zhang K, Li FS, Zhang K, Koros WJ (2014) Gas separation performance of carbon molecular sieve membranes based on 6FDA-mPDA/DABA (3:2) polyimide. ChemSusChem 7:1186–1194

53. Hosseini SS, Chung TS (2009) Carbon membranes from blends of PBI and polyimides for N$_2$/CH$_4$ and CO$_2$/CH$_4$ separation and hydrogen purification. J Membr Sci 328:174–185

54. Askari M, Yang T, Chung TS (2012) Natural gas purification and olefin/paraffin separation using cross-linkable dual-layer hollow fiber membranes comprising b-cyclodextrin. J Membr Sci 423–424:392–403

55. Davison J, Thambimuthu K (2004) Technologies for capture of carbon dioxide. In: Proceedings of the seventh greenhouse gas technology conference, Vancouver, Canada. International Energy Association (IEA), Greenhouse Gas R&D Progamme www.ghght7.ca

56. Ryckebosch E, Drouillon M, Vervaeren H (2011) Techniques for transformation of biogas to biomethane. Biomass Bioenergy 35:1633–1645

57. Favre E (2007) Carbon dioxide recovery from post-combustion processes: can gas permeation membranes compete with absorption? J Membr Sci 294:50–59

58. Papadias D, Ahmed S, Kumar R (2012) Fuel quality issues with biogas energy e an economic analysis for a stationary fuel cell system. Energy 44:257–277